

Discovery of a Brain-Penetrant S1P₃-Sparing Direct Agonist of the S1P₁ and S1P₅ Receptors Efficacious at Low Oral Dose

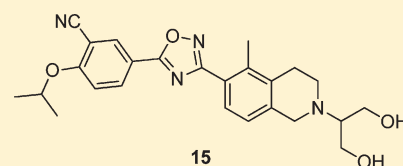
Emmanuel H. Demont,^{*,†} Sandra Arpino,[‡] Rino A. Bit,[†] Colin A. Campbell,[†] Nigel Deeks,[†] Sapna Desai,[‡] Simon J. Dowell,[‡] Pam Gaskin,[†] James R. J. Gray,[†] Lee A. Harrison,[†] Andrea Haynes,[†] Tom D. Heightman,[‡] Duncan S. Holmes,[‡] Philip G. Humphreys,[†] Umesh Kumar,[†] Mary A. Morse,[†] Greg J. Osborne,[‡] Terry Panchal,[†] Karen L. Philpott,[‡] Simon Taylor,[†] Robert Watson,[†] Robert Willis,[†] and Jason Witherington[†]

[†]Immuno Inflammation Center of Excellence for Drug Discovery, [‡]Platform Technology and Science, GlaxoSmithKline, Gunnels Wood Road, Stevenage SG1 2NY, United Kingdom

[‡]Neurology Center of Excellence for Drug Discovery, GlaxoSmithKline, New Frontiers Science Park, Third Avenue, Harlow, Essex CM19 5AW, United Kingdom

S Supporting Information

ABSTRACT: 2-Amino-2-(4-octylphenethyl)propane-1,3-diol **1** (fingolimod, FTY720) has been recently marketed in the United States for the treatment of patients with relapsing remitting multiple sclerosis (RRMS). Its efficacy has been primarily linked to the agonism on T cells of S1P₁, one of the five sphingosine 1-phosphate (S1P) G-protein-coupled receptors, while its cardiovascular side effects have been associated with activity at S1P₃. Emerging data suggest that the ability of this molecule to cross the blood-brain barrier and to interact with both S1P₁ and S1P₅ in the central nervous system (CNS) may contribute to its efficacy in treating patients with RRMS. We have recently disclosed the structure of an advanced, first generation S1P₃-sparing S1P₁ agonist, a zwitterion with limited CNS exposure. In this Article, we highlight our strategy toward the identification of CNS-penetrant S1P₃-sparing S1P₁ and S1P₅ agonists resulting in the discovery of 5-(3-{2-[2-hydroxy-1-(hydroxymethyl)ethyl]-5-methyl-1,2,3,4-tetrahydro-6-isoquinolinyl}-1,2,4-oxadiazol-5-yl)-2-[(1-methyl)oxy]benzonitrile **15**. Its exceptional *in vivo* potency and good pharmacokinetic properties translate into a very low predicted therapeutic dose in human (<1 mg p.o. once daily).



S1P₁ pEC₅₀ (β-arrestin) = 8.5
S1P₃ pEC₅₀ (GTPγS) < 4.4
S1P₅ pEC₅₀ (Aequorin) = 7.7
In vivo IC₅₀ < 0.1 nM
Rat [Br] : [BI] = 1.87 : 1

INTRODUCTION

2-Amino-2-(4-octylphenethyl)propane-1,3-diol (**1**) (Fingolimod, FTY720, Figure 1)¹ has been recently marketed in the United States for the treatment of patients with relapsing remitting multiple sclerosis (RRMS). Administration of **1** leads to the sequestration of lymphocytes in secondary lymphoid organs and consequently to a reduction of lymphocyte count in the peripheral blood. **1** is phosphorylated *in vivo* by sphingosine kinase-2^{2,3} to form FTY720-P **2**, a potent agonist of four of the five G-protein-coupled receptors (S1P₁, S1P₃₋₅) associated with the lysolipid sphingosine 1-phosphate (S1P) **3**. Agonism of the S1P₁ receptor by S1P is required to induce egress of T cells from lymphoid organs and **2** acts as a functional antagonist by internalizing the receptor.^{4,5} The cardiovascular side effects observed in treated patients (bradycardia and hypertension) have been linked to partial agonism of the S1P₃ receptor,^{6,7} although more recent findings from human studies indicate that S1P₁ may mediate the transient effects on heart rate.⁸ Owing to its lipophilic nature, **1** is able to cross the blood-brain barrier (BBB)⁹ where **2** interacts with S1P receptors present on astrocytes (S1P₁) and on oligodendrocytes (S1P₅). Recent publications suggest this may play a role in fingolimod's efficacy in the treatment of patients with RRMS.^{10,11}

Understanding of the unique mode of action of **1** has triggered intensive effort toward the discovery of S1P₁ agonists with increased selectivity versus S1P₃,¹² either as pro-drugs such as CS-0777¹³ **4** or direct agonists such as ACT-128800¹⁴ **5** (Figure 2).

Excellent (>1000 fold) selectivity over S1P₃ can be achieved with agonists such as AMG 369¹⁵ **6** or PF-991¹⁶ **7**, but these molecules, as our own S1P₃-sparing agonist **8**¹⁷ (Table 1), are zwitterions and are therefore likely to have poor CNS penetration.¹⁸ Typically, in our hands, **8** proved to be a P-gp substrate (with an efflux ratio in a human MDR1 transfected MDCK type 2 cell line of 0.5 and 6.0 in the presence and absence of a P-gp inhibitor, respectively). Interestingly, **8** shows no activity at S1P₂ and S1P₄, and is a partial agonist of the S1P₅ receptor with similar potency to that at S1P₁.¹⁹

RESULTS AND DISCUSSION

Agonists such as **8** are interesting because molecules with an identical triaryl core are in clinical trials^{20,21} (not as S1P₁ agonists), suggesting good developability properties. We decided to use this template in order to identify agonists with increased brain

Received: May 13, 2011

Published: August 15, 2011

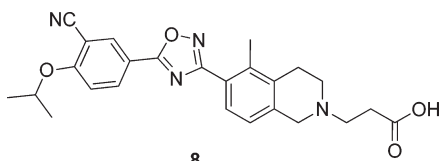
penetration versus **8**. Due to the plethora of amines known to be able to cross the BBB, and thanks to the intrinsic activity of compounds such as **9** (Table 2) at S1P₁, we decided to use **9** as starting point, knowing that the removal of the acid functionality should enhance CNS penetration.¹⁸ The profile of **9** suggested the main liabilities associated with analogous molecules would be related to (1) hERG inhibition, (2) risk of phospholipidosis²² with such cationic amphiphilic structure, and (3) long pharmacokinetic (PK) half-life of compounds with moderate clearance and high volume of distribution. This could lead to accumulation on chronic dosing and long pharmacodynamic (PD) half-life.

As previously highlighted,¹⁷ our strategy focused on drug-ability, seeking CNS penetrant agonists in a chemical space recently identified as minimizing the risk of toxicological findings in the clinic (cLogP < 3, polar surface area (PSA) > 75).²³ We considered that lowering the pK_a of our compounds compared to **9**, while also lowering their lipophilicity (assessed by cLogP) with the addition of hydrophilic polar substituents, was likely to discharge the phospholipidosis and hERG-related cardiovascular risks highlighted above, even if it may have an impact on CNS penetration.^{18,24} Lowering pK_a and cLogP should reduce the volume of distribution (V_{ss}) of our agonists; for a given in vivo clearance, this would lead to a shorter PK half-life and lower the risk of accumulation on chronic dosing, therefore offering better reversibility of the lymphopenia in patients, in sharp contrast to **1**.

We embarked on the generation of an array of S1P₁ agonists using a range of bicyclic amines (benzazepines, benzoxazepines, THIQ, and aza-THIQ) of different pK_a bearing hydrophilic substituents such as amides or polyhydroxylated side chains. The chemistry used is highlighted in Scheme 1: Protected bicyclic amines bearing a nitrile substituent were reacted with hydroxylamine, and the corresponding hydroxyamidines were coupled to acid chloride **11** (for which the substitution pattern

was known to be the best compromise between MW, cLogP and S1P₁ activity from previous SAR)¹⁷ to form the central

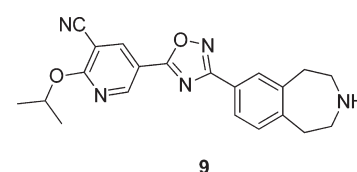
Table 1. Activity of **2** and **8** at S1P₁₋₅ Receptors



human receptor (assay) ^a	pEC ₅₀ (maximum activation %)	
	2 ^b	8
S1P ₁ (β-arrestin)	7.7 (99), n = 44	8.25 (94), n = 13
S1P ₂ (yeast)	<4.5, n = 5	<4.48 (01), n = 6
S1P ₃ (GTPγS)	8.3 (62), n = 38	<4.5 (35), n = 6
S1P ₄ (aequorin)	6.7 (48), n = 2	<4.38 (03), n = 4
S1P ₅ (aequorin)	7.2 (62), n = 2	6.79 (77), n = 6

^a See the Supporting Information for details. ^b For comparative published values, see ref 35.

Table 2. Profile of Lead Amine **9**



MW, cLogP, PSA	375, 3.6, 97
CHI LogD @ pH 2.0, 7.4, 10.5	1.34, 2.65, 3.73
CAD-likeness	91
measured pK _a	9.69
S1P ₁ pEC ₅₀ (β-arrestin)	7.7
S1P ₃ pEC ₅₀ (GTPγS)	<4.5
hERG pIC ₅₀ (Dofetilide)	5.5
fraction unbound (rat, %)	0.25
rat PK	
CLb (mL/min/kg) ^a	20
V _{ss} (L/kg) ^a	9.7
t ^{1/2} (h) ^a	6.3
F p.o. (%) ^b	70

^a 1 mg/kg i.v. ^b 3 mg/kg p.o.

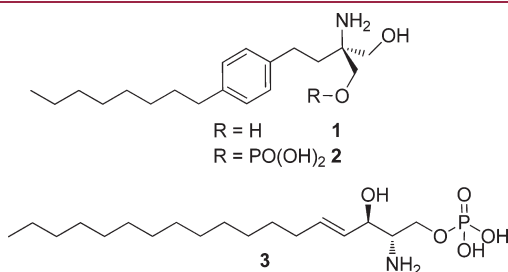


Figure 1. Structure of FTY720 **1**, its phosphate **2**, and S1P **3**.

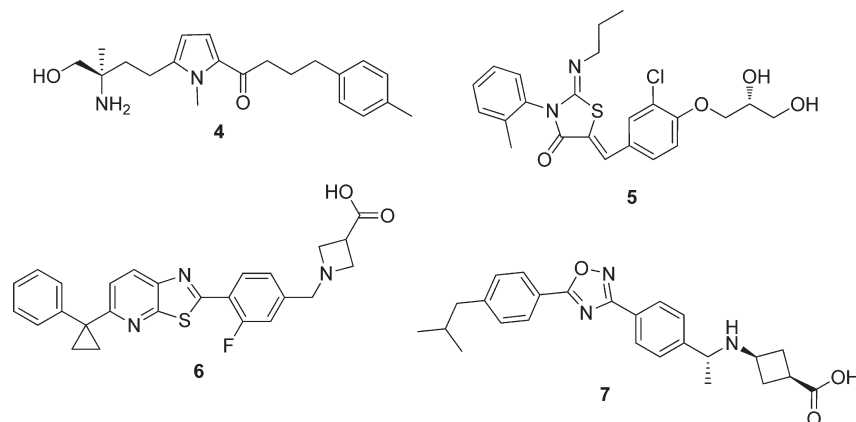
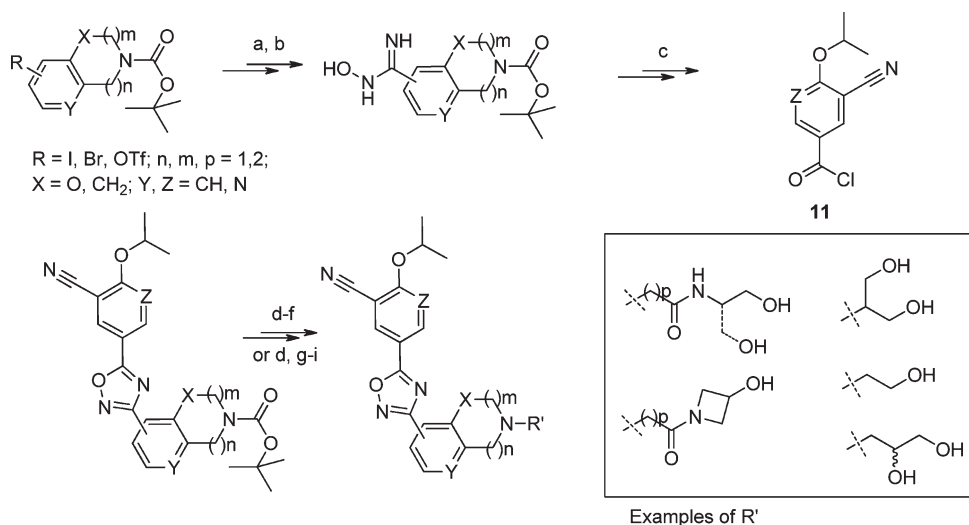


Figure 2. Structure of known S1P₁ agonists.

Scheme 1. Synthesis of Nonacidic Biaryl Oxadiazole S1P₁ Agonists^a

^a Reagents and conditions: (a) Zn(CN)₂, Pd(PPh₃)₄, DMF, 100 °C; (b) aqueous NH₂OH, EtOH, 80 °C; (c) **11**, pyridine, toluene, 0 to 110 °C; (d) HCl, dioxane, room temperature; (e) R₃R₄CO, CH₂Cl₂, room temperature then NaBH(OAc)₃; (f) HCl, THF, room temperature; (g) Br-(CH₂)_n-COOR₅, K₂CO₃, CH₃CN, 50 °C; (h) NaOH, EtOH, room temperature; (i) HATU, *N*-ethyl-*N*-isopropylpropan-2-amine (DIPEA), DMF/NMP, HNR₆R₇, room temperature.

oxadiazole. After deprotection, well precedented chemistry (alkylation, saponification, amide coupling, or reductive amination) allowed the introduction of the appropriate side chain (see representative examples in Scheme 1).

The nature of the side chain had little impact on the S1P₁ activity, and most of the compounds made had a pEC₅₀ similar to or better than that of **9** in our primary assay with good (>100 fold) or excellent (>1000 fold) selectivity against S1P₃. The diversity of the analogues made helped us to identify the drivers of the three parameters we wanted to modify: (1) As shown in Figure 3, lipophilicity (measured by chromatographic hydrophobicity index LogP (CHI LogP))²⁵ had an impact on the cationic amphiphilic drug (CAD)-likeness of our molecules, a parameter linked to phospholipidosis,²⁶ and lowering the lipophilicity tended to lower the CAD-likeness of our molecules. However, the correlation was poor for molecules having a CHI LogP in the area we were targeting (CHI LogP < 3).

The key parameter influencing CAD-likeness appeared to be the basicity of the amines screened (Figure 4): the lower the pK_a, the lower the CAD-likeness, and amines with pK_a < 7.5 were therefore targeted.

(2) The basicity of the amine also had an impact on the ability to distribute into tissue (Figure 5), and amines with a pK_a < 7.5 had the highest probability of having a Vss in rats considered unlikely to lead to accumulation on chronic dosing. Lipophilicity (cLogP, CHI LogD) or PSA had lower impact on the tissue distribution (see graphics in Experimental Section).

(3) Tuning the pK_a and/or the lipophilicity had only a small, nonpredictable effect on hERG inhibition (Figure 6), and most compounds showed IC₅₀ in a 1–20 μM range in a PatchXpress assay; the good in vivo activity of these molecules (vide infra) and their high protein binding (>95% in all cases; see **9**, Table 2 as example) led us to believe a significant safety margin might be achieved.

Table 3 highlights the in vitro and in vivo potency and selectivity as well as in vivo pharmacokinetics of key representatives. Compounds with amide side chains such as **10** were

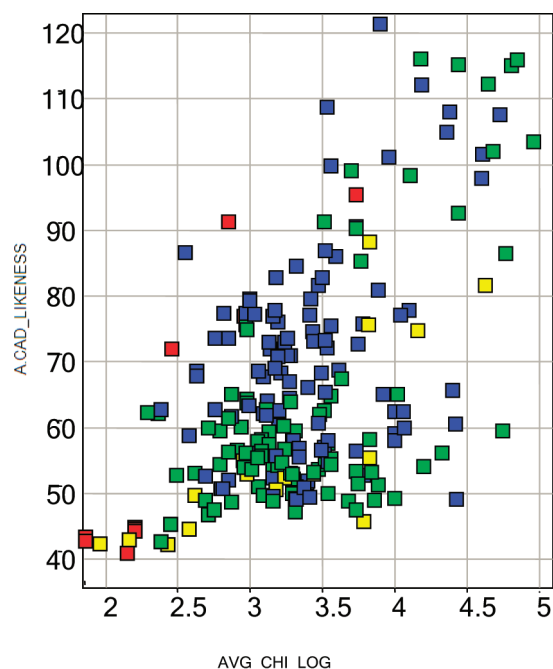


Figure 3. Correlation between CHI LogP and CAD-likeness for a set of benzazepine (blue), THIQ (green), AZA-THIQ (red), and benzoxazepine (yellow) for CHI LogP < 5 and CAD-likeness < 120.

efficacious in our in vivo lymphopenia assay at an oral dose of 1 mg/kg, but further analysis showed that they were readily hydrolyzed to the corresponding acid in vivo. Not only is this metabolite responsible for part of the PD effect observed, but it generated the same potential toxicity risk associated with our first generation agonist **8** (formation of acyl-glucuronide).²⁷ The formation of the acid could be avoided with hindered amides, but this led to molecules outside of the targeted chemical space (cLogP < 3) and no further work was done in this area.

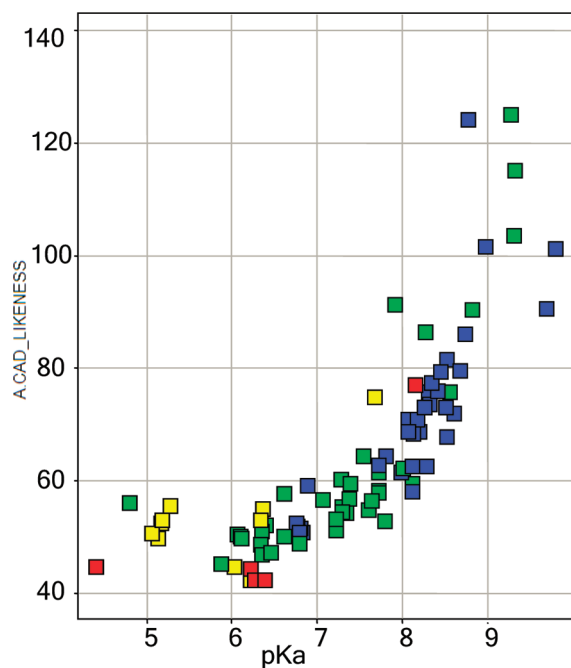


Figure 4. Correlation between CAD-likeness and measured pK_a .

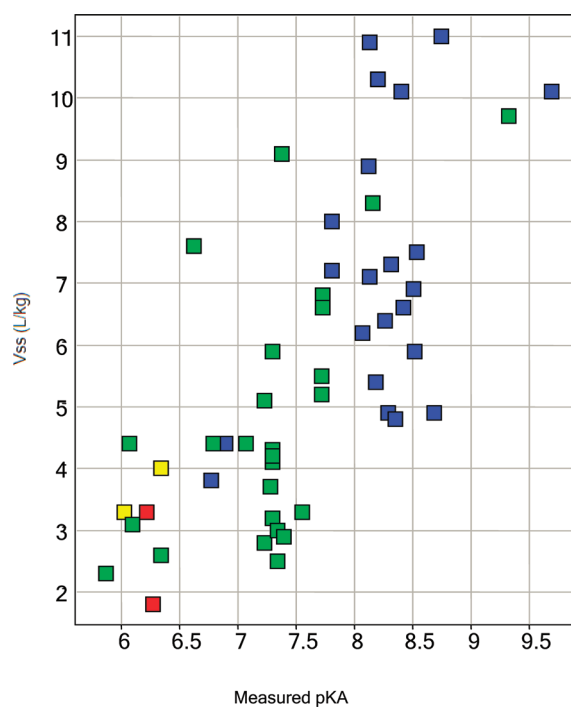


Figure 5. Correlation between volume of distribution in rats and measured pK_a .

Derivatives with hydroxylated side chains, diols in particular, proved interesting (see profiles of **11**–**15**). Benzazepines (**11**) had low in vivo clearance but were too basic, leading to a high V_{ss} . The less basic benzazepines had lower V_{ss} but despite good in vivo PK were less potent in our lymphopenia model (cf. **12** vs **11**). The analogous THIQ (**15**) had overall the best profile: It proved more efficacious in vivo (at doses as low as 0.3 mg/kg p.o., vide infra) and had appropriate intrinsic properties (CHI LogD, pK_a ,

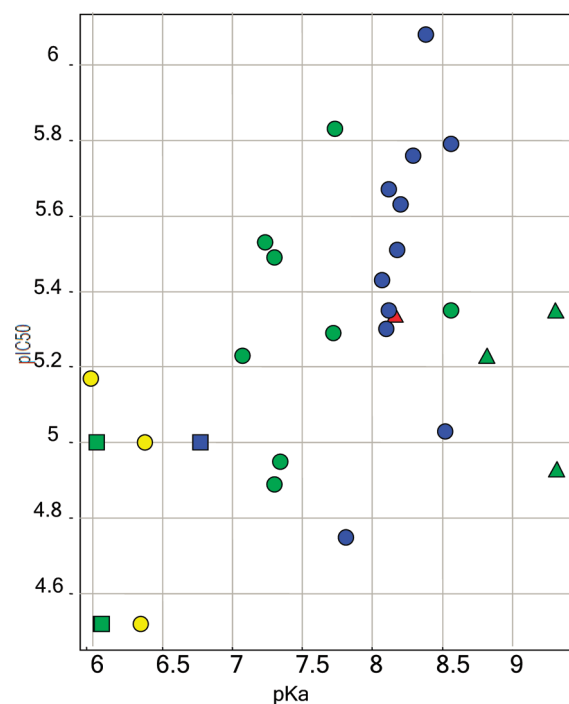


Figure 6. Correlation between hERG PatchXpress pIC_{50} and measured pK_a .

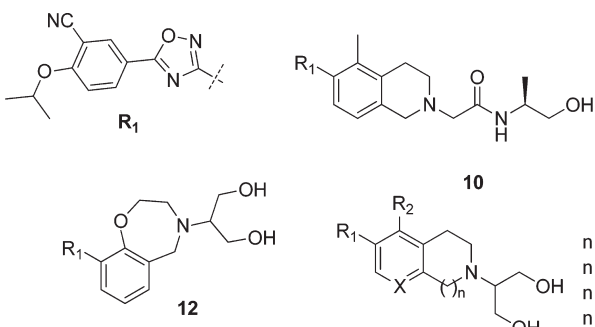
V_{ss} , and CAD-likeness). Introduction of a methyl substituent ortho to the oxadiazole in this series gave improved S1P₃ selectivity and lower in vivo clearance in rats (cf. **15** vs **14**). Attempts to further lower the pK_a and lipophilicity by introduction of nitrogen into the aromatic ring (**13**) led to compounds with lower V_{ss} , but all were less efficacious in vivo.

The synthesis of compound **15** is highlighted in Scheme 2: enone **17** was obtained from commercial protected piperidone **16** via a Robinson annulation then was oxidized to phenol **18** using a Saegusa reaction. Palladium mediated cyanation via triflate **19** gave **20** which was then reacted with hydroxylamine. The hydroxyamidine **21** was then coupled to acid chloride **22** (obtained from the corresponding commercially available acid), and oxadiazole **23** was obtained after dehydration of the uncyclized intermediate. Deprotection in acidic conditions (**24**) followed by reductive amination (**25**) and deprotection of the acetal provided **15**.

Similar chemistry was used to access compounds **9**–**14**, using the corresponding (hetero)aryl nitriles **28**, **30**, **33**, and **38**. Their synthesis is highlighted in Scheme 3. Nitrile **28** and **30** could be easily accessed via palladium mediated cyanation from commercial bromide **26** and known²⁸ phenol **29**, respectively. The synthesis of the benzazepine template started with known²⁹ aldehyde **31**, which after reductive amination using ethanolamine and protection of the secondary amine gave **32**. The ring was formed using a Mitsunobu reaction to give **33** after cyanation. The aza-THIQ template was obtained following amination of the beta-keto ester **35** (obtained from commercial benzyl derivative **34**) followed by imine formation and ring closure in basic conditions which gave the aryl bromide **37**. The latter was converted to the desired intermediate **38** via a Suzuki coupling.

Full lymphopenia could be achieved with **15** at doses as low as 0.3 mg/kg p.o. with reversibility within 24 h (Figure 7). PK/PD modeling using an indirect response model estimated an in vivo

Table 3. In Vitro and in Vivo Profile of Selected Agonists



compd	10	11	12	13	14	15
MW, cLogP, PSA	490, 2.7, 125	449, 3.3, 116	451, 2.7, 125	450, 2.2, 129	434, 2.5, 116	449, 3.0, 116
CHI LogD @ pH 7.4	3.04	2.74	2.41	2.00	2.49	2.64
CAD-likeness	50	64	45	44	60	55
measured pK _a	6.07	7.81	6.03	6.22	7.28	7.30
SIP ₁ pEC ₅₀ (β-arrestin)	8.9 (2)	7.7 (8)	7.7 (2)	7.7 (8)	8.1 (6)	8.5 (54)
SIP ₃ pEC ₅₀ (GTPγS)	4.6 (1)	4.8 (3)	<4.5 (2)	<4 (10)	5.2 (4)	<4.5–5.5 (47) ^a
maximum lymphopenia (±SD) @ 1 mg/kg p.o.	90 ± 3	88 ± 3	60 ± 13	70 ± 3	49 ± 12	96 ± 4
hERG pIC ₅₀ (max inh % @ 30 μM, PatchXpress)	<5 (43)	4.75 (59)	5.17 (77)	4.9 ^b	4.7 ^b	4.89 (58)
rat PK						
(n = 1–3)						
CLb (mL/min/kg) ^c	32	21 ± 3	14	21	87	60 ± 6
V _{ss} (L/kg) ^c	4.4	7.6 ± 0.4	3.3	3.3	3.7	4.1 ± 0.5
t ¹ / ₂ (h) ^c	2.0	5.3 ± 0.3	3.5	2.1	0.6	1.0 ± 0.1
F _i p.o. (%)	38 ± 17 ^e	68 ± 18 ^c		37 ± 18 ^e		52 ± 4 ^d
ratio AUC acid:amide	2.3:1					

n = 2, X = CH, R₂ = H **11**
n = 1, X = N, R₂ = CH₃ **13**
n = 1, X = CH, R₂ = H **14**
n = 1, X = CH, R₂ = CH₃ **15**

^a In 33 occasions, pEC₅₀ < 4.5; in 14 occasions, 4.5 < pEC₅₀ < 5.5; in all cases, maximum response <40% at 30 μM. ^b Dofetilide. ^c 1 mg/kg i.v. DMSO/10% (w/v) kleptose HPB 0.9% saline (aqueous) (5%:95% v/v). ^d 3 mg/kg p.o. 1% (w/v) methylcellulose 400 (aqueous). ^e 1 mg/kg p.o. 1% methylcellulose.

IC₅₀ of less than 0.1 nM. There were no active metabolites or phosphorylated adducts observed systemically which could explain such a level of potency. This increased in vivo potency compared to our first generation zwitterionic agonists may be attributed to an increased distribution into tissues: **15** not only can desensitize T cells to S1P by internalizing SIP₁ but it may also play a role in the tightening of the lymphatic endothelial cell junctions, a mode of action also hypothesized to explain fingolimod's efficacy.³⁰

Due to these promising data, further profiling of **15** was implemented. This compound has excellent intrinsic properties (Table 5), solubility, and permeability. No significant CYP inhibition was observed, and no covalent adducts were detected in glutathione trapping experiments (nor time dependent inhibition of CYP 3A4). In vitro hepatocyte clearance correlated with in vivo clearance in rat and dog. Oral bioavailability was good in both species. As for **8**, **15** proved to be a partial agonist at SIP₅, with similar EC₅₀ as for SIP₁. The permeability of **15** was assessed in MDCKII-MDR1 cells. The basolateral-apical (B–A) to A–B ratio was unaffected by the presence or absence of a P-gp inhibitor, indicating that the transport of this agonist was not affected by efflux transporters, in contrast to zwitterion **8**. A CNS penetration study in rats demonstrated that **15** was able to enter the CNS with a brain to blood ratio concentration at steady state of 1.85:1. The capacity of **15** to cross the BBB could be considered as surprising given its PSA (116 Å²) is higher than what is considered as upper limit for good CNS penetration (PSA < 70 Å²).³¹ The intrinsic properties of **15** are also different

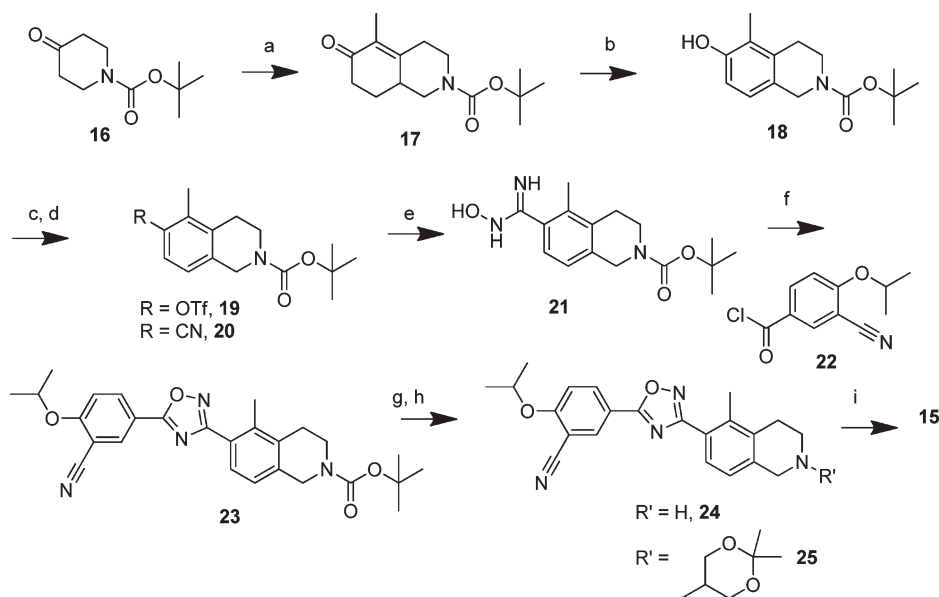
from those of marketed CNS drugs (median MW = 305, number of hydrogen bond donor = 1).³² The higher than expected CNS penetration of **15** maybe in part due to its excellent permeability which could be due to formation of an intramolecular hydrogen bond. This phenomenon has already been observed with other templates.³³ Overall, a review of the literature shows that the “hot spot” in the chemical space for CNS penetration is not exclusive and that other molecules with similar profile to **15** can be CNS penetrant.³⁴

CONCLUSION

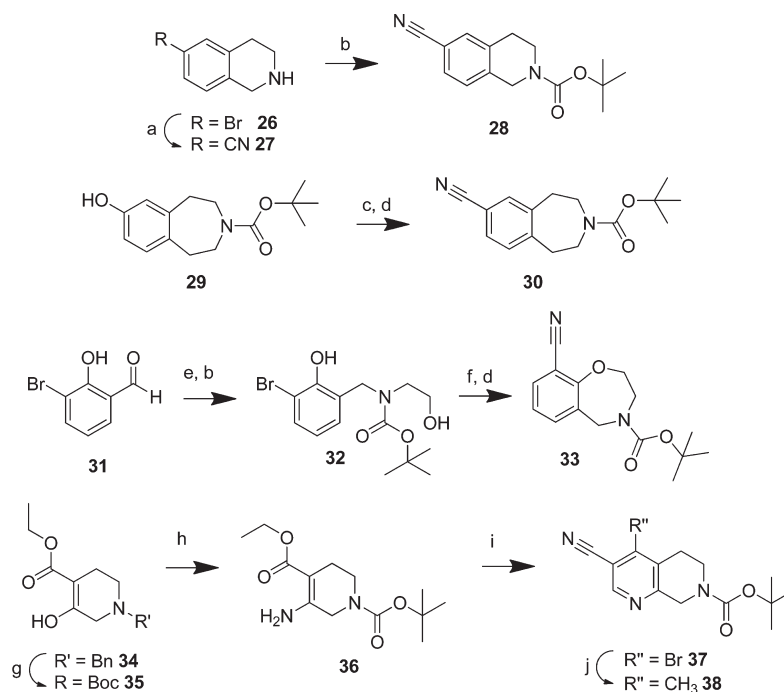
We have identified a druglike CNS-penetrant SIP₃-sparing direct (non-pro-drug) agonist of the SIP₁ and SIP₅ receptors showing exceptional in vivo efficacy (IC₅₀ < 0.1 nM). Its good pharmacokinetic properties suggest very low human therapeutic doses (<1 mg p.o. once daily).

EXPERIMENTAL SECTION

General. All solvents were purchased from Romil Ltd. (Hy-Dry anhydrous solvents), and commercially available reagents were used as received. Melting points were recorded on a Buchi B-545 apparatus and are uncorrected. All reactions were followed by TLC analysis (TLC plates GF254, Merck) or LCMS (liquid chromatography mass spectrometry) using a Waters ZQ instrument. NMR spectra were recorded on a Bruker AVANCE 400 spectrometer and are referenced as follows: ¹H (400 MHz), internal standard TMS at δ = 0.00; ¹³C (100.6 MHz), internal standard CDCl₃ at δ = 77.23 or DMSO-*d*₆ at δ = 39.70. Column

Scheme 2. Synthesis of Compound 15^a

^a Reagents and conditions: (a) (i) Pyrrolidine, toluene, Dean–Stark, reflux; (ii) 1-penten-3-one, hydroquinone, toluene, reflux. (b) (i) LiHMDS, THF, $-63\text{ }^{\circ}\text{C}$ then TMSCl; (ii) CH_3CN , $\text{Pd}(\text{OAc})_2$, $T < 35\text{ }^{\circ}\text{C}$ then TBAF, room temperature; (c) pyridine, $(\text{CF}_3\text{SO}_2)_2\text{O}$, CH_2Cl_2 , $-35\text{ }^{\circ}\text{C}$. (d) $\text{Zn}(\text{CN})_2$, $\text{Pd}(\text{PPh}_3)_4$, DMF, $100\text{ }^{\circ}\text{C}$. (e) $\text{NH}_2\text{OH}\cdot\text{HCl}$, K_2CO_3 , ethanol, reflux; (f) **22**, toluene/pyridine, room temperature to $110\text{ }^{\circ}\text{C}$; (g) HCl, 1,4-dioxane, room temperature; (h) 2,2-dimethyl-1,3-dioxan-5-one, CH_2Cl_2 , room temperature then $\text{NaHB}(\text{OAc})_3$; (i) HCl, THF/water, room temperature.

Scheme 3. Synthesis of Key Benzonitrile Intermediates^a

^a Reagents and conditions: (a) $\text{Zn}(\text{CN})_2$, $\text{Pd}(\text{PPh}_3)_4$, DMF, microwave irradiations, $130\text{ }^{\circ}\text{C}$; (b) $(\text{Boc})_2\text{O}$, NEt_3 , CH_2Cl_2 , room temperature; (c) pyridine, $(\text{CF}_3\text{SO}_2)_2\text{O}$, CH_2Cl_2 , $-35\text{ }^{\circ}\text{C}$; (d) $\text{Zn}(\text{CN})_2$, $\text{Pd}(\text{PPh}_3)_4$, DMF, $90\text{ }^{\circ}\text{C}$; (e) ethanolamine, THF, $0\text{ }^{\circ}\text{C}$ then $\text{NaHB}(\text{OAc})_3$, $0\text{ }^{\circ}\text{C}$ to room temperature; (f) PPh_3 , DIAD, THF, $0\text{ }^{\circ}\text{C}$; (g) H_2 (1 atm), Pd/C , ethanol, $(\text{Boc})_2\text{O}$, room temperature; (h) NH_4OAc , ethanol, room temperature to $50\text{ }^{\circ}\text{C}$; (i) 3,3-dimethoxypropionitrile, $t\text{-BuOK}$, THF, 0 to $70\text{ }^{\circ}\text{C}$ then PBr_3 , DMF/ CH_2Cl_2 , $0\text{ }^{\circ}\text{C}$; (j) $\text{CH}_3\text{BF}_3\text{K}$, $\text{PdCl}_2(\text{dppf})$, Cs_2CO_3 , THF/water, $65\text{ }^{\circ}\text{C}$.

chromatography was performed on prepacked silica gel columns (30–90 mesh, IST) using a biotage SP4. Mass spectra were recorded

on Waters ZQ (ESI-MS) and Q-ToF 2 (HRMS) spectrometers. Mass Directed Auto Prep was performed on a Waters 2767 instrument with a

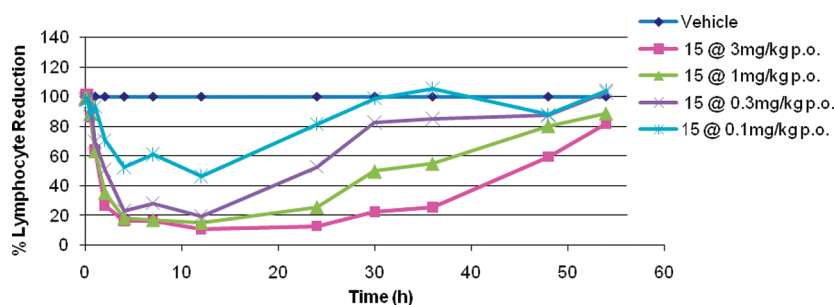


Figure 7. Lymphocyte reduction over time in rats following oral administration of 15.

Table 5. In Vitro Profile of 15

MW, PSA, cLogP		449, 116, 3.0
CHI LogD @ pH 2.0, 7.4 and 10.5		0.98; 2.64; 2.99
SIP ₅ pEC ₅₀ (max response %; n = 5)		7.7 ± 0.17 (65–67%)
solubility (FeSSIF, ng/mL)		>1000
permeability (MDCK Type 2, nm/s)		175
hepatocyte CLi (mL/min/g; rat, dog, mouse, cyno, human)		3; 30; 1.3; 1.3; 2
CYP IC ₅₀ (μM, 2C9, 2C19, 2D6, 3A4VG, 3A4 VR, n = 2)		4.3; >50; >50; 8.4; 15.3
steady state rat [brain]:[blood] ^{a,b} (n = 3)		1.87:1 ± 0.02:1
dog PK (1 mg/kg i.v. ^b or p.o. ^c ; n = 1)	CLb (mL/min/kg) ^b	29
	V _{ss} (L/kg) ^b	7.0
	t _{1/2} (i.v., h) ^b	3.0
	F, p.o. % ^c	45

^a 7 h i.v. dose at 0.8 mg/kg/h. ^b DMSO/10% (w/v) Kleptose HPB 0.9% saline (aq) (2:98 v/v). ^c 1% (w/v) methylcellulose 400 (aq).

MicroMass ZQ mass spectrometer using a Supelco LCABZ++ column. GLOBAL gradients for chromatography are as follows (solvent B polar component, CV = column volume). 10% GLOBAL: 3% B for 2 CV, 3 to 13% B over 10 CV then 13% B for 5 CV; 20% GLOBAL: 5% B for 2 CV, 5 to 20% B over 10 CV then 20% B for 5 CV; 30% GLOBAL: 8% B for 2 CV, 8 to 38% B over 10 CV then 38% B for 5 CV; 40% GLOBAL: 10% B for 2 CV, 10 to 50% B over 10 CV then 50% B for 5 CV; 50% GLOBAL: 13% B for 2 CV, 13 to 63% B over 10 CV then 63% B for 5 CV. 100% GLOBAL: 25% B for 2 CV, 25 to 100% B over 10 CV then 100% B for 10 CV. Abbreviations for multiplicities observed in NMR spectra: s, singlet; br s, broad singlet; d, doublet; t, triplet; q, quadruplet; p, pentuplet; spt, septuplet; m, multiplet. All compounds reported are of at least 95% purity according to LCMS (conditions described in the Experimental Section).

1,1-Dimethylethyl 5-Methyl-6-oxo-3,4,6,7,8,8a-hexahydro-2(1H)-isoquinolinecarboxylate (17). Compound 16 (70 g, 350 mmol, Aldrich) and pyrrolidine (43.6 mL, 530 mmol) were dissolved in toluene (310 mL), and the resulting mixture was refluxed under Dean–Stark conditions for 24 h and then concentrated in vacuo. The residue was dissolved in anhydrous toluene (270 mL) and treated with hydroquinone (0.40 g) and 1-penten-3-one (29.6 g, 350 mmol). The resulting solution was refluxed for 24 h and then diluted with AcOEt (300 mL). The mixture was washed with HCl (0.5 N in water, 500 mL), and the aqueous phase extracted with AcOEt (300 mL). The combined organic phases were dried (MgSO₄) and concentrated. Purification of the residue by flash chromatography on a silica cartridge (1.5 kg) gave the title compound (55.2 g, 59.2%) as a pale yellow oil which crystallized on standing. LCMS (method formate): Retention time 1.04 min, [M + H]⁺ = 266.24. ¹H NMR (400 MHz, CDCl₃) δ ppm 4.16–4.02 (m, 2H), 3.08–3.01 (m, 1H), 2.77–2.71 (m, 1H), 2.58–2.49 (m, 3H), 2.39–2.26 (m, 2H), 2.06–2.00 (m, 1H), 1.79 (s, 3H), 1.59–1.52 (m, 1H), 1.49 (s, 9H).

1,1-Dimethylethyl 6-Hydroxy-5-methyl-3,4-dihydro-2(1H)-isoquinolinecarboxylate (18). Lithium bis(trimethylsilyl)amide (1 M in THF, 246 mL, 250 mmol) was added dropwise to a solution of compound 17 (54.4 g, 210 mmol) in THF (200 mL) at –63 °C, and the mixture was stirred for an additional 30 min. Chloro(trimethyl)silane (31.4 mL, 250 mmol) was added dropwise, and the resulting mixture was stirred for 2 h at –70 °C. The reaction was warmed to room temperature over 20 min and diluted with Et₂O (800 mL). The reaction was added to a saturated Na₂CO₃ aqueous solution, and the phases were separated. The aqueous phase was extracted with Et₂O (300 mL) and the combined organic phases were dried (Na₂SO₄) and concentrated in vacuo. The residue was dissolved in acetonitrile (200 mL), and palladium(II) acetate (46.0 g, 210 mmol) was added. The resulting mixture was cooled (water bath) to maintain a reaction temperature below 35 °C and stirred for 16 h. The reaction was filtered through Celite, and the residue rinsed with AcOEt (3 × 300 mL). The filtrate was further filtered through a 1'' pad of silica gel and concentrated in vacuo. The residue was dissolved in AcOEt (500 mL) and then treated with tetrabutylammonium fluoride (1 M in THF, 200 mL, 200 mmol). The resulting mixture was allowed to stand for 30 min, then was washed with HCl (0.5 N in water, 300 mL) and a 10% sodium thiosulfate solution, dried (MgSO₄), and concentrated in vacuo. Purification of the residue by flash chromatography on silica gel (300 g column) eluting with 0–60% gradient AcOEt/cyclohexane gave the title compound (29.9 g, 55%) as a white solid. LCMS (method formate): Retention time 1.07 min, [M + H]⁺ = 264.12. ¹H NMR (400 MHz, DMSO-*d*₆) δ ppm 9.03 (s, 1H), 6.75 (d, J = 8.1 Hz, 1H), 6.64 (d, J = 8.1 Hz, 1H), 4.36 (s, 2H), 3.52 (t, J = 6.1 Hz, 2H), 2.62 (t, J = 6.1 Hz, 2H), 2.01 (s, 3H), 1.41 (s, 9H). HRMS calculated for C₁₅H₂₂NO₃: 264.1600. Found: 264.1605.

1,1-Dimethylethyl 5-Methyl-6-[[[(trifluoromethyl)sulfonyl]oxy]-3,4-dihydro-2(1H)-isoquinolinecarboxylate (19). To a

solution of compound **18** (3.16 g, 12 mmol) in dichloromethane (50 mL) at room temperature under nitrogen was added pyridine (1.94 mL, 24 mmol), and the resulting solution was cooled to -30°C before trifluoromethanesulfonic anhydride (2.2 mL, 13.2 mmol) was added dropwise. The resulting mixture was stirred for 40 min at this temperature, warmed to room temperature, and concentrated in vacuo. The residue was diluted with AcOEt and washed sequentially with HCl (1 N in water), a saturated NaHCO_3 aqueous solution, and brine. The organic phase was then dried over MgSO_4 and concentrated in vacuo to give the title compound (4.85 g, 102%) as a red oil which was used in the next step without further purification. LCMS (method high pH): Retention time 1.46 min, $[\text{M} - \text{H}]^- = 394.22$. ^1H NMR (400 MHz, CDCl_3) δ ppm 7.10 (d, $J = 8.1$ Hz, 1H), 7.02 (d, $J = 8.1$ Hz, 1H), 4.58 (s, 2H), 3.68 (t, $J = 5.8$ Hz, 2H), 2.76 (t, $J = 5.8$ Hz, 2H), 2.25 (s, 3H), 1.50 (s, 9H).

1,1-Dimethylethyl 6-Cyano-5-methyl-3,4-dihydro-2(1H)-isoquinolinecarboxylate (20). A solution of compound **19** (26.1 g, 66 mmol) in DMF (200 mL) was degassed for 10 min under vacuum and then flushed with nitrogen. The solution was treated with tetrakis-(triphenylphosphine)palladium (7.6 g, 6.6 mmol) and zinc cyanide (10.1 g, 86 mmol), and the resulting mixture was stirred at 100°C under nitrogen for 6 h and then was cooled to room temperature. The mixture was filtered, the residue washed with AcOEt, and most of the solvent evaporated in vacuo. The residue was dissolved in AcOEt, and the organic phase was washed twice with a saturated NaHCO_3 aqueous solution. The combined aqueous phases were extracted twice with AcOEt, and the combined organic phases were washed with brine, dried over MgSO_4 , and concentrated in vacuo. Purification of the residue by flash chromatography on silica gel eluting with a 0–50% AcOEt/cyclohexane gradient gave the title compound (16.6 g, 92%) as a white solid. LCMS (method high pH): Retention time 1.24 min, $[\text{M} + \text{H}]^+ = 273.25$. ^1H NMR (400 MHz, $\text{DMSO}-d_6$) δ ppm 7.57 (d, $J = 8.1$ Hz, 1H), 7.22 (d, $J = 8.1$ Hz, 1H), 4.56 (s, 2H), 3.59 (t, $J = 6.1$ Hz, 2H), 2.72 (t, $J = 6.1$ Hz, 2H), 2.39 (s, 3H), 1.44 (s, 9H). HRMS calculated for $\text{C}_{16}\text{H}_{21}\text{N}_2\text{O}_2$: 273.1603. Found: 273.1608.

1,1-Dimethylethyl 6-[(Hydroxyamino)(imino)methyl]-5-methyl-3,4-dihydro-2(1H)-isoquinolinecarboxylate (21). A mixture of compound **20** (16.6 g, 61 mmol), NaHCO_3 (30.7 g, 370 mmol), and hydroxylamine hydrochloride (25.4 g, 370 mmol) in ethanol (250 mL) was refluxed for 28 h and then was allowed to cool to room temperature. The reaction was filtered, and the residue washed with ethanol. The combined filtrate and washings were concentrated in vacuo. The residue was poured into water (100 mL) and stirred at room temperature for 20 min. The precipitated solid was isolated by filtration and dried under vacuum at 40°C for 16 h to give the title compound (16 g, 86%) as a white solid. LCMS (method high pH): Retention time 0.93 min, $[\text{M} + \text{H}]^+ = 306.17$. ^1H NMR (400 MHz, $\text{DMSO}-d_6$) δ ppm 9.21 (s, 1H), 7.07 (d, $J = 8.9$ Hz, 1H), 6.99 (d, $J = 8.9$ Hz, 1H), 5.65 (s, 2H), 4.48 (s, 2H), 3.58 (t, $J = 5.9$ Hz, 2H), 2.67 (t, $J = 5.9$ Hz, 2H), 2.20 (s, 3H), 1.43 (m, 9H). HRMS calculated for $\text{C}_{16}\text{H}_{24}\text{N}_3\text{O}_3$: 306.1818. Found: 306.1817.

3-Cyano-4-[(1-methylethyl)oxy]benzoyl Chloride (22). Oxalyl chloride (6.4 mL, 73 mmol) was added to a solution of 3-cyano-4-[(1-methylethyl)oxy]benzoic acid (10.7 g, 52 mmol, Biopharma Inc.) in CH_2Cl_2 (100 mL) followed by the addition of DMF (0.044 mL, 0.57 mmol), and the resulting mixture was stirred at room temperature for 4 h. The reaction mixture was filtered and concentrated in vacuo. The residue was coevaporated with cyclohexane (2×50 mL) to give the title compound (11.7 g, 100%) as a pale yellow oil which solidified on standing.

1,1-Dimethylethyl 6-(5-{3-Cyano-4-[(1-methylethyl)oxy]phenyl}-1,2,4-oxadiazol-3-yl)-5-methyl-3,4-dihydro-2(1H)-isoquinolinecarboxylate (23). To a suspension of compound **21** (4.6 g, 15 mmol) in toluene (30 mL) and pyridine (30 mL) at room temperature under nitrogen was slowly added compound **22** (3.5 g,

16 mmol) in toluene (15 mL). After 15 min, the resulting mixture was refluxed for 90 min (internal temperature 110°C) and then was cooled to room temperature. The solution was decanted from the brown precipitate, the precipitate washed with toluene, and the combined organics concentrated in vacuo. The residue was dissolved in AcOEt, and the resulting solution washed with HCl (2 N in water). The aqueous phase was extracted with AcOEt, and the combined organic phases were washed sequentially with a saturated NaHCO_3 aqueous solution and brine, dried over MgSO_4 , and concentrated in vacuo. Purification of the residue on SP4 using a 30% GLOBAL gradient (AcOEt in hexanes) gave the title compound (3.62 g, 51%) as a white foam. LCMS (method high pH): Retention time 1.55 min, $[\text{M} + \text{H}]^+ = 475.31$. ^1H NMR (400 MHz, CDCl_3) δ ppm 8.42 (d, $J = 2.3$ Hz, 1H), 8.33 (dd, $J = 8.8, 2.3$ Hz, 1H), 7.76 (d, $J = 8.1$ Hz, 1H), 7.16–7.08 (m, 2H), 4.79 (spt, $J = 6.1$ Hz, 1H), 4.64 (s, 2H), 3.72 (t, $J = 5.8$ Hz, 2H), 2.84 (t, $J = 5.8$ Hz, 2H), 2.52 (s, 3H), 1.51 (s, 9H), 1.48 (d, $J = 6.1$ Hz, 6H).

2-[(1-Methylethyl)oxy]-5-[3-(5-methyl-1,2,3,4-tetrahydro-6-isoquinolinyl)-1,2,4-oxadiazol-5-yl]benzotrile hydrochloride (24). To a solution of compound **23** (3.4 g, 7.2 mmol) in 1,4-dioxane (20 mL) at room temperature under nitrogen was added HCl (4 N in 1,4-dioxane, 18 mL, 72 mmol), and the resulting mixture was stirred at this temperature for 5.5 h, stored in a freezer for 16 h, and then concentrated in vacuo. The residue was coevaporated with Et_2O to give the title compound (2.88 g, 98%) as a white solid. LCMS (method high pH): Retention time 1.21 min, $[\text{M} + \text{H}]^+ = 375.26$. ^1H NMR (400 MHz, $\text{DMSO}-d_6$) δ ppm 9.54 (br s, 2H), 8.50 (d, $J = 2.2$ Hz, 1H), 8.39 (dd, $J = 9.0, 2.2$ Hz, 1H), 7.77 (d, $J = 8.1$ Hz, 1H), 7.56 (d, $J = 9.0$ Hz, 1H), 7.29 (d, $J = 8.1$ Hz, 1H), 4.98 (spt, $J = 6.1$ Hz, 1H), 4.35 (s, 2H), 3.45 (t, $J = 6.1$ Hz, 2H), 3.00 (t, $J = 6.1$ Hz, 2H), 2.47 (s, 3H), 1.39 (d, $J = 6.1$ Hz, 6H). HRMS calculated for $\text{C}_{22}\text{H}_{23}\text{N}_4\text{O}_2$: 375.1821. Found: 375.1817.

5-(3-(2-(2,2-Dimethyl-1,3-dioxan-5-yl)-5-methyl-1,2,3,4-tetrahydroisoquinolin-6-yl)-1,2,4-oxadiazol-5-yl)-2-isopropoxybenzotrile (25). Sodium triacetoxylborohydride (3.56 g, 16.8 mmol) was added portionwise over 30 min to a stirred suspension of compound **24** (1.5 g, 3.65 mmol) and 2,2-dimethyl-1,3-dioxan-5-one (1.43 g, 11 mmol) in dry dichloromethane (50 mL). The reaction mixture was then stirred at room temperature for 4 h. A saturated aqueous NaHCO_3 solution (50 mL) was added carefully (CARE: gas evolved), and the resulting biphasic mixture stirred vigorously for 30 min. The layers were separated, and the aqueous phase was extracted with DCM (2×20 mL). The combined organic phases were dried over MgSO_4 and concentrated in vacuo to give the title compound (1.80 g, 3.65 mmol, 100%) as a colorless solid which was used in next step without further purification. LCMS (method high pH): Retention time 0.94 min, $[\text{M} + \text{H}]^+ = 488.9$.

5-(3-(2-(1,3-Dihydroxypropan-2-yl)-5-methyl-1,2,3,4-tetrahydroisoquinolin-6-yl)-1,2,4-oxadiazol-5-yl)-2-isopropoxybenzotrile hydrochloride (15). A solution of compound **25** (1.78 g, 3.65 mmol) in THF (50 mL) was treated with HCl (2 N in water, 50 mL, 100 mmol), and the resulting mixture was stirred at room temperature for 16 h. Most of the THF was removed in vacuo. The residue was neutralized by the portionwise addition of solid NaHCO_3 (CARE: gas evolved). During neutralization, a colorless solid precipitated which was filtered off and dissolved in 10% methanol in DCM (50 mL). The solution was dried over MgSO_4 then concentrated in vacuo. The residue was dissolved in methanol (~ 10 mL) and treated with HCl (1 N in Et_2O , 4 mL, 4 mmol). Et_2O (100 mL) was then added to the solution. The precipitated formed was filtered off, washed with Et_2O , and dried under vacuum to give the title compound (1.47 g, 3 mmol, 83%) as a colorless solid. LCMS (method high pH): Retention time 0.89 min, $[\text{M} + \text{H}]^+ = 449.05$. ^1H NMR (400 MHz, $\text{DMSO}-d_6$) δ ppm 10.58 (br s, 1H), 8.52 (d, $J = 2.2$ Hz, 1H), 8.42 (dd, $J = 9.2, 2.2$ Hz, 1H), 7.81 (d, $J = 8.1$ Hz, 1H), 7.59 (d, $J = 9.2$ Hz, 1H), 7.31 (d, $J = 8.1$ Hz,

1H), 5.54 (br s, 2H), 5.01 (spt, $J = 6.1$ Hz, 1H), 4.78 (dd, $J = 15.8, 8.3$ Hz, 1H), 4.62 (d, $J = 15.8$ Hz, 1H), 4.01–3.90 (m, 5H), 3.65–3.55 (m, 1H), 3.47–3.43 (m, 1H), 3.28–3.19 (m, 1H), 3.18–3.09 (m, 1H), 2.50 (s, 3H), 1.42 (d, $J = 6.1$ Hz, 6H). ^{13}C NMR (DMSO- d_6) δ ppm 173.0, 169.0, 162.5, 136.0, 134.5, 133.7, 132.1, 131.9, 128.0, 125.2, 124.6, 115.9, 115.2, 114.9, 102.4, 72.5, 66.6, 56.9, 56.7, 50.7, 47.4, 23.9, 21.4, 16.2. HRMS calculated for $\text{C}_{25}\text{H}_{29}\text{N}_4\text{O}_4$: 449.2189. Found: 449.2194.

■ ASSOCIATED CONTENT

S Supporting Information. Experimental procedures for the synthesis of compounds **9–14**, in vitro assay protocols for the determination of EC_{50} , and protocols for in vivo studies and data correlations. This material is available free of charge via the Internet at <http://pubs.acs.org>.

■ AUTHOR INFORMATION

Corresponding Author

*Telephone: + 44 1438 764319. Fax: + 44 1438 768302. E-mail: emmanuel.h.demont@gsk.com.

■ ACKNOWLEDGMENT

The authors thank Dr. Richard Upton and Mr. Nick Waite for NMR support, Dr. Bill Leavens for recording HRMS spectra, Mrs. Helen Tracey for conducting P-gp and permeability experiments, Mrs. Catherine Cartwright and Miss Aarti Patel for determining intrinsic clearance, and Mrs. Karen Leavens for supporting the lymphopenia studies. Mrs. Shenaz Nunhuck and Mr. Alan Hill are also acknowledged for pK_a and CHI determination, and Miss Helen Garden for solubility measurements.

■ ABBREVIATIONS

RRMS, remitting relapsing multiple sclerosis; CNS, central nervous system; BBB, blood-brain barrier; PSA, polar surface area; CHI, chromatographic hydrophobicity index; CAD, cationic amphiphilic drug; LiHMDS, lithium bis(trimethylsilyl)amide; TMSCl, chloro(trimethyl)silane; DIAD, diisopropyl diazene-1,2-dicarboxylate; GPCR, G-protein-coupled receptor

■ REFERENCES

- (1) Martini, S.; Peters, H.; Böhrer, T.; Budde, K. Current Perspectives on FTY720. *Expert Opin. Invest. Drugs* **2007**, *16*, 505–518.
- (2) Billich, A.; Bormancin, F.; Dévay, P.; Mechtcheriakova, D.; Urtz, N.; Baumruker, T. Phosphorylation of the Immunomodulatory Drug FTY720 by Sphingosine Kinases. *J. Biol. Chem.* **2003**, *278*, 47408–47415.
- (3) Albert, R.; Hinterding, K.; Brinkmann, V.; Guerini, D.; Müller-Hartwig, C.; Knecht, H.; Simeon, C.; Streiff, M.; Wagner, T.; Welzenbach, K.; Zécéri, F.; Zollinger, M.; Cooke, N.; Francotte, E. Novel Immunomodulator FTY720 Is Phosphorylated in Rats and Humans to Form a Single Stereoisomer. Identification, Chemical Proof, and Biological Characterisation of the Biologically Active Species and Its Enantiomer. *J. Med. Chem.* **2005**, *48*, 5373–5377.
- (4) Matloubian, M.; Lo, C. G.; Cinamon, G.; Lesneski, M. J.; Xu, Y.; Brinkmann, V.; Allende, M. L.; Proia, R. L.; Cyster, J. G. Lymphocyte egress from thymus and peripheral lymphoid organs is dependent on S1P receptor 1. *Nature* **2004**, *427*, 355–360.
- (5) Wei, S. H.; Rosen, H.; Matheu, M. P.; Sanna, M. G.; Wang, S.-K.; Jo, E.; Wong, C.-H.; Parker, I.; Cahalan, M. D. Sphingosine 1-Phosphate Type 1 receptor Agonism Inhibits Transendothelial Migration of Medullary T Cells to Lymphatic Sinuses. *Nat. Immunol.* **2005**, *6*, 1228–1235.

- (6) Forrest, M.; Sun, S.-Y.; Hajdu, R.; Bergstrom, J.; Card, D.; Doherty, G.; Hale, J.; Keohane, C.; Meyers, C.; Milligan, J.; Mills, S.; Nomura, N.; Rosen, H.; Rosenbach, M.; Shei, G.-J.; Singer, I. I.; Tian, M.; West, S.; White, V.; Xie, J.; Proia, R. L.; Mandala, S. Immune Cell Regulation and Cardiovascular Effects of Sphingosine 1-Phosphate Receptor Agonists in Rodents Are Mediated via Distinct Receptor Subtypes. *J. Pharmacol. Exp. Ther.* **2004**, *309*, 758–768.

- (7) Sanna, M. G.; Liao, J.; Jo, E.; Alfonso, C.; Ahn, M.-Y.; Peterson, M. S.; Webb, B.; Lefebvre, S.; Chun, J.; Gray, N.; Rosen, H. Sphingosine 1-Phosphate (S1P) Receptor Subtypes S1P₁ and S1P₃, Respectively, Regulate Lymphocyte Recirculation and Heart Rate. *J. Biol. Chem.* **2004**, *279*, 13839–13848.

- (8) Gergely, P.; Wallström, E.; Nuesslein-Hildesheim, B.; Bruns, C.; Zécéri, F.; Cooke, N.; Traebert, M.; Tuntland, T.; Rosenberg, M.; Saltzman, M. Phase I study with selective S1P₁/S1P₅ receptor modulator BAF312 indicates that S1P₁ rather than S1P₃ mediates transient heart rate reduction in humans. *Mult. Scler.* **2009**, *15*, S31–S150.

- (9) Meno-Tetang, G. M. L.; Li, H.; Mis, S.; Pyszczynski, N.; Heining, P.; Lowe, P.; Jusko, W. J. Physiologically based pharmacokinetic modeling of FTY720 (2-amino-2[2-(4-octylphenyl)ethyl]propane-1,3-diol hydrochloride) in rats after oral and intravenous doses. *Drug Metab. Dispos.* **2006**, *34*, 1480–1487.

- (10) Brinkmann, V. FTY720 (fingolimod) in Multiple Sclerosis: therapeutic effects in the immune and the central nervous system. *Br. J. Pharmacol.* **2009**, *158*, 1173–1182.

- (11) Noguchi, K.; Chun, J. Roles for lysophospholipid S1P receptors in multiple sclerosis. *Crit. Rev. Biochem. Mol. Biol.* **2011**, *46*, 2–10.

- (12) Buzard, D. J.; Thatte, J.; Lerner, M.; Edwards, J.; Jones, R. M. Recent Progress in the Development of Selective S1P₁ Receptor Agonists for the Treatment of Inflammatory and Autoimmune disorders. *Expert Opin. Ther. Pat.* **2008**, *18*, 1141–1159.

- (13) Nishi, T.; Miyazaki, S.; Takemoto, T.; Suzuki, K.; Iio, Y.; Nakajima, K.; Ohnuki, T.; Kawase, Y.; Nara, F.; Inaba, S.; Izumi, T.; Yuita, H.; Oshima, K.; Doi, H.; Inoue, R.; Tomisato, W.; Kagari, T.; Shimozato, T. Discovery of CS-0777: A Potent, Selective, and Orally Active S1P₁ Agonist. *ACS Med. Chem. Lett.* **2011**, *2*, 368–372.

- (14) Bolli, M. H.; Abele, S.; Binkert, C.; Bravo, R.; Buchmann, S.; Bur, D.; Gatfield, J.; Hess, P.; Kohl, C.; Mangold, C.; Mathys, B.; Menyhart, K.; Müller, C.; Nayler, O.; Scherz, M.; Schmidt, G.; Sippel, V.; Steiner, B.; Strasser, D.; Treiber, A.; Weller, T. 2-Imino-thiazolidin-4-one Derivatives as Potent, Orally Active S1P₁ Receptor Agonists. *J. Med. Chem.* **2010**, *53*, 4198–4211.

- (15) Cee, V. J.; Frohn, M.; Lanman, B. A.; Golden, J.; Muller, K.; Neira, S.; Pickrell, A.; Arnett, H.; Buys, J.; Gore, A.; Fiorino, M.; Horner, M.; Itano, A.; Lee, M. R.; McElvain, M.; Middleton, S.; Schrag, M.; Rivenzon-Segal, D.; Vargas, H. M.; Xu, H.; Xu, Y.; Zang, X.; Siu, J.; Wong, M.; Bürl, R. W. Discovery of AMG 369, a Thiazolo[5,4-b]pyridine Agonist of S1P₁ and S1P₅. *ACS Med. Chem. Lett.* **2011**, *2*, 107–112.

- (16) Walker, J. K. Discovery of a potent and selective S1P₁ receptor agonist for the treatment of rheumatoid arthritis. ACS meeting, 21–25 March, 2010, San Francisco, CA.

- (17) Demont, E. H.; Andrews, B. I.; Bit, R. A.; Campbell, C. A.; Cooke, J. W. B.; Deeks, N.; Desai, S.; Dowell, S. J.; Gaskin, P.; Gray, J. R. J.; Haynes, A.; Holmes, D. S.; Kumar, U.; Morse, M. A.; Osborne, G. J.; Panchal, T.; Patel, B.; Perboni, A.; Taylor, S.; Watson, R.; Witherington, J.; Willis, R. Discovery of a selective S1P₁ receptor agonist efficacious at low oral dose and devoid of effects on heart rate. *ACS Med Chem. Lett.* **2011**, *2*, 444–449.

- (18) Didziapetris, R.; Japertas, P.; Avdeef, A.; Petrauskas, A. Classification Analysis of P-Glycoprotein Substrate Specificity. *J. Drug Targeting* **2003**, *11*, 391–406.

- (19) Such a selectivity profile has already been reported with this biaryl oxadiazole template. See: Li, Z.; Chen, W.; Hale, J. J.; Lynch, C. L.; Mills, S. G.; Hajdu, R.; Keohane, C. A.; Rosenbach, M. J.; Milligan, J. A.; Shei, G.-J.; Chrebet, G.; Parent, S. A.; Bergstrom, J.; Card, D.; Forrest, M.; Quackenbush, E. J.; Wickham, L. A.; Vargas, H.; Evans, R. M.; Rosen, H.; Mandala, S. Discovery of Potent 3,5-Diphenyl-1,2,4-oxadiazole

Sphingosine-1-Phosphate-1 (S1P₁) Receptor Agonists with Exceptional Selectivity against S1P₂ and S1P₃. *J. Med. Chem.* **2005**, *48*, 6169–6173.

(20) Feigin, V. Irampanel. *Curr. Opin. Invest. Drugs* **2002**, *3*, 908–910.

(21) Hirawat, S.; Welch, E. M.; Elfring, G. L.; Northcutt, V. J.; Paushkin, S.; Hwang, S.; Leonard, E. M.; Almstead, N. G.; Ju, W.; Peltz, S. W.; Miller, L. L. Safety, Tolerability, and Pharmacokinetics of PCT124, a Nonaminoglycoside Nonsense Mutation Suppressor, Following Single- and Multiple-Dose Administration to Healthy Male and Female Adult Volunteers. *J. Clin. Pharmacol.* **2007**, *47*, 430–444.

(22) Reasor, M. J.; Hastings, K. L.; Ulrich, R. G. Drug-induced phospholipidosis: issues and future direction. *Expert Opin. Drug. Saf.* **2006**, *5*, 567–583.

(23) Hughes, J. D.; Blagg, J.; Price, D. A.; Bailey, S.; DeCrescenzo, G. A.; Devraj, R. V.; Ellsworth, E.; Fobian, Y. M.; Gibbs, M. E.; Gilles, R. W.; Greene, N.; Huang, E.; Krieger-Burke, T.; Loesel, J.; Wager, T.; Whiteley, L.; Zhang, Y. Physicochemical Drug Properties Associated With In Vivo Toxicological Outcomes. *Bioorg. Med. Chem. Lett.* **2008**, *18*, 4872–4875.

(24) Van De Waterbeemd, H.; Camenisch, G.; Folkers, G.; Chretien, J. R.; Raevsky, O. A. Estimation of Blood-Brain Barrier Crossing of Drugs Using Molecular Size and Shape, and H-bonding Descriptors. *J. Drug Targeting* **1998**, *6*, 151–165.

(25) Valkó, K.; Bevan, C.; Reynolds, D. Chromatographic Hydrophobicity Index by Fast-Gradient RP-HPLC: A High-Throughput Alternative to log P/log D. *Anal. Chem.* **1997**, *69*, 2022–2029.

(26) Monteith, D. K.; Morgan, R. E.; Halstead, B. In vitro assays and biomarkers for drug-induced phospholipidosis. *Expert Opin. Drug. Metab. Toxicol.* **2006**, *2*, 687–696.

(27) Kalgutkar, A. S.; Gardner, I.; Obach, R. S.; Shaffer, C. L.; Callegari, E.; Henne, K. R.; Mutlib, A. E.; Dalvie, D. K.; Lee, J. S.; Nakai, Y.; O'Donnell, J. P.; Boer, J.; Harriman, S. P. A comprehensive listing of bioactivation pathways of organic functional groups. *Curr. Drug Metab.* **2005**, *6*, 161–225.

(28) Hadley, M. S.; Lightfoot, A. P.; MacDonald, G. J.; Stemp, G. Tetrahydrobenzodiazepine derivatives useful as modulators of dopamine D3 receptors (antipsychotic agents). PCT Int. Appl. WO200240471A1, 2002.

(29) Hansen, T. V.; Skattelboel, L. Ortho-formylation of phenols: preparation of 3-bromosalicylaldehyde. *Org. Synth.* **2005**, *82*, 64–68.

(30) Marsolais, D.; Rosen, H. Chemical modulators of sphingosine-1-phosphate receptors as barrier-oriented therapeutic molecules. *Nat. Rev. Drug Discovery* **2009**, *8*, 297–307.

(31) Norinder, U.; Haerberlein, M. Computational approaches to the prediction of the blood-brain distribution. *Adv. Drug Delivery Rev.* **2002**, *54*, 291–313.

(32) Wager, T. T.; Villalobos, A.; Verhoest, P. R.; Hou, X.; Shaffer, C. L. Strategies to optimize the brain availability of central nervous system drug candidates. *Expert Opin. Drug Discovery* **2011**, *6*, 371–381.

(33) Ashwood, V. A.; Field, M. J.; Horwell, D. C.; Julien-Larose, C.; Lewthwaite, R. A.; McCleary, S.; Pritchard, M. C.; Raphy, J.; Singh, L. Utilization of an intramolecular hydrogen bond to increase the CNS penetration of an NK1 receptor antagonist. *J. Med. Chem.* **2001**, *44*, 2276–2285.

(34) Hitchcock, S. A.; Pennington, L. D. Structure-brain exposure relationships. *J. Med. Chem.* **2006**, *49*, 7559–7583.

(35) Brinkmann, V.; Davis, M. D.; Heise, C. E.; Albert, R.; Cottens, S.; Hof, R.; Bruns, C.; Prieschl, E.; Baumruker, T.; Hiestand, P.; Foster, C. A.; Zollinger, M.; Lynch, K. R. The immune modulator FTY720 targets sphingosine 1-phosphate receptors. *J. Biol. Chem.* **2002**, *277*, 21453–21457.